Food Chemistry: X 27 (2025) 102464

Contents lists available at ScienceDirect

Food Chemistry: X

journal homepage: www.sciencedirect.com/journal/food-chemistry-x

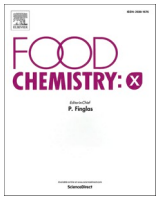

Effects of different fruit freeze-dried powders on the 3D printing properties of peach gum-based gummy candy gels

Ye-Xing Liang [a], Jing-Bing Xu [c], Li Zhou [b], Xue Li [a], Ling Zhang [a,*], Fan-Bing Meng [b,d,*]

[a] Agricultural Product Processing Institute, Chongqing Academy of Agricultural Science, Chongqing 401329, PR China
[b] College of Food and Biological Engineering, Chengdu University, Chengdu 610106, PR China
[c] Chongqing Institute for Food and Drug Control, Chongqing 401121, PR China,
[d] Sichuan Kelun Pharmaceutical Co., Ltd, Chengdu 610072, PR China

ARTICLE INFO

Keywords:
Peach gum polysaccharides
3D printing
Rheology
Rheological properties
Fruit composite gel

ABSTRACT

The rheological properties and 3D printing effects of different composite gels were explored, and the results revealed that the viscosity of the peach gum polysaccharide and gelatin composite gel (PGP/GE)was moderate, and had the best 3D printing quality and stability. Using PGP/GE as the 3D printing substrate and adding five types of freeze-dried fruit powders. Strawberries, mangoes, and yellow peaches had better water binding abilities than sea buckthorn and mulberries did; as the amount of fruit powder added increased, its ability to bind water increased. The 3D printing quality of mulberries and sea buckthorn was inferior to that of yellow peaches, strawberries, and mangoes. The printing effect of the low-dose fruit powder groups (5 g, 16.67 % w/v) were better than those of the high-dose groups (10 g, 33.33 % w/v). Through texture and sensory analysis, the low-dose fruit powder groups had better taste, especially the low-dose strawberry compound gel group.

1. Introduction

Recently, 3D printing technology has become a research focus in the food industry. This approach can save processing time, and reduce resource consumption and production costs, which can provide novel customized food manufacturing methods on the basis of customer preferences for food size and sensory and nutritional characteristics. For example, 3D printing technology can create soft food for dysphagic older people (Yu et al., 2023) and can also be employed for making shaped food with multiple nutrients to benefit picky children. 3D food printing materials are crucial because they need to flow easily during extrusion to form the desired shape and structure, and must also support structural integrity after printing, however, because these two characteristics are often contradictory, the material resources for high-quality 3D bio-printing are still limited (Jiang et al., 2022).

Polysaccharide hydrocolloids have high gel properties, and can undergo extrusion molding qualities under appropriate conditions. Therefore, they can serve as 3D printing materials (Sharma et al., 2024). Adding an appropriate amount of polysaccharide hydrocolloids can improve mechanical strength after 3D printing and increase the stability of the model shape of the printing products, which allows 3D printing to produce more refined and complex food gels. Gelatin, k-carrageenan and low-acyl gellan gum have been verified to be used as 3D printing materials in natural polysaccharide gels. However, single natural polysaccharide gels have defects, for example, gelatin has poor thermal stability and gellan gum has poor elasticity. Therefore, many studies have improved thermal stability and effectiveness of 3D printing materials through adding multiple gel mixtures or protein. For example, gum arabic, guar gum, k-carrageenan, and xanthan gum had significant effects on the 3D printing behavior of the orange juice wheat starch mixture (Azam et al., 2018).

Peach gum (PG) is a type of natural plant gum obtained from peach trees. The natural sources of PG are abundant and easy to obtain, it exceeds 10 billion tons per year in China alone, but only a small portion of the gum has been utilized, so currently, the utilization rate of PG is very low, resulting in large amounts of waste (Zeng et al., 2022). Recent studies have shown that peach gum polysaccharide (PGP) has various physiological functions, such as lowering blood sugar, slowing aging, reducing oxidative stress, and enhancing immunity (Licá et al., 2018), therefore, PG has potential application value in the food, medicine, and cosmetics industries. Generally, PG is prepared via the hydrolysis method to obtain PGP. The PGP solution has shear thinning characteristics, which has similar properties to gum arabic. The PGP solution can maintain high viscosity at 25–80 °C. At the same concentration, the

* Corresponding authors.
E-mail addresses: jdteazl@163.com (L. Zhang), mfb1020@163.com (F.-B. Meng).

https://doi.org/10.1016/j.fochx.2025.102464
Received 28 October 2024; Received in revised form 12 April 2025; Accepted 14 April 2025
Available online 15 April 2025

viscosity of PGP is consistently higher than that of gum arabic (Zeng et al., 2022), These features can accurately compensate for the defects of some 3D-printed substrates. Therefore, we tried to add PGP to prepare composite gels for 3D printing in the study.

In recent years, the diet problem of high fat, high sugar, high sodium, low fruits and vegetables has become the main dietary structure problem. Fruits can provide various nutrients to the human body. Therefore, the application of fruit materials 3D printing is important for the development of personalized nutritional foods. But the composition of different fruit powder is quite different. Comparative study on the 3D printing effect of different fruit powder to select the materials suitable for 3D printing. It has great significance for the industrial production of 3D printing fruit powder gummy candy.

In this work, PGPs were combined with κ-carrageenan, gelatin or gellan gum to explore their gel properties and to identify the most suitable printing substrate composite gel agent. On the basis of composite gel, a preliminary study on the 3D printing of fruit powder as a food source by adding freeze-dried fruit powder was performed to explore the relationships between the rheological and textural properties of printing systems with different types and masses of freeze-dried fruit powder. The aim of this study was to select fruit powder sources for food 3D-printed formulas and provide a reference for the optimization of 3D printing process parameters. Ultimately, the goal was to expand the market application of PG and promote comprehensive utilization of PG.

2. Materials and methods

2.1. Materials

High fructose corn syrup was purchased from Xiangchijiangyuan Biotechnology Co. Ltd. (Shandong, China). Peach gum was purchased from Anhui Youtai Bioengineering Co., Ltd. (Anhui, China). Gelatin (B type) was procured from Yuanye Biotechnology Co., Ltd. (Shanghai, China). k-carrageenan and low-acyl gellan gum were purchased from Shanghai McLean Biochemical Technology Co., Ltd. (Shanghai, China). Freeze-dried powders of strawberry, mulberry, mango, yellow peach, and sea buckthorn were purchased from Sichuan Jin Sifang Fruit Industry Co., Ltd. (Sichuan, China). The total pectin content detection kit was purchased from Beijing Soleibao Technology Co., Ltd. (Beijing, China); the other chemical reagents were of analytical grade.

2.2. Preparation of PGP

PG (100 g) was dispersed in 4 L of ultrapure water and soaked at room temperature for 24 h, stirred at 90 °C for 2 h, cooled to 25 °C, centrifuged at 4000 ×*g* for 20 min. Collected supernatant , added 4 times the volume of ethanol (Sun et al., 2022), the obtained precipitates were lyophilized to obtain PGP, which was crushed into a powder (100 mesh). According to the previous detection methods (Li, Du, et al., 2021), the average molecular weight of PGP is 1.47×10^7 g/mol.

2.3. Selection of the substrate composite gel for 3D printing

2.3.1. Preparation of the composite gel solution

First, high fructose corn syrup (10 g) was first dissolved in 100 mL of ultrapure water. 5 % PGP was added, and the mixture was dissolved thoroughly with stirring for 30 min at 60 °C. Finally, 1.5 % k-carrageenan, 1.5 % gellan gum, or 6 % gelatin were added to separate beakers of dissolved PGP solution with stirring for 30 min, and the beaker mouths were covered with plastic wrap during the heating process. After full dissolution, the solutions were degassed with an ultrasonic degasser for 2 min, and the PGP/KC, PGP/GG, and PGP/GE composite gel solutions were obtained.

2.3.2. Rheological measurements

In accordance with Zhong et al. (Zhong et al., 2018), a rheometer (Anton Paar MCR302e, Germany) equipped with a pendulum (28 mm in diameter) and a cup (30 mm in diameter) was used for the rheological measurements, 10 mL of sample was added, and steady shearing analysis was conducted at shear rates ranging from 0.1 s^{-1} to 100 s^{-1} at 25 °C.

Linear viscoelastic region (LVER) was obtained via strain sweep (30 °C, 1 Hz) within the strain range of 0.1 % to 1000 %. All subsequent oscillation tests were performed within the LVER. The frequency scans were performed in the frequency range from 0.1 Hz to 100 Hz, and at 25 °C and 0.5 % strain.

The temperature sweep tests were conducted at 0.5 % strain at a frequency of 1 Hz. The cooling temperature ranged from 80 °C to 5 °C at a rate of 5 °C/min, and maintain a constant temperature of 5 °C was maintained for 10 min. The heating stage ranged from 5 °C to 80 °C, with a heating rate of 5 °C/min (Abedinia et al., 2017).

2.3.3. 3D printing process

The gel solutions, which were prepared in 2.3.1, were injected into a 3D printer (Kunshan PORIMY 3D Printing Technology Co., Ltd., Jiangsu, China). A heart-shaped body (length 45 mm, width 45 mm, height 15 mm) was used to evaluate printability. The parameters were set as follows: layer height,1 mm; temperature, 25 °C; nozzle movement speed, 20 mm/s; nozzle diameter, 1.55 mm; and syringe size, 5 cm in diameter and 20 cm in height. The printing accuracy was calculated via Eq. (1) by measuring the diagonal length and height of the printing products (Fan et al., 2020)。

$$\text{Printing accuracy} = \frac{\text{Measured value for product}}{\text{Target value for setting}} \times 100\% \quad (1)$$

2.3.4. LF-NMR and SEM analysis

The ^{1}H-T_2 relaxation of the samples was tested via a low-field pulsed NMR (LF-NMR) analyzer (MesoMR20–040 V-I, Suzhou. China). The Carr–Purcell–Meiom–Gill sequence was used, and the parameters were as follows: CPMG: CPMG: SF, 19 MHz; P1, 5.6; P2, 9.2; O1, 45 Hz; TW, 15000 ms; SW, 5000 KHz; RFD, 0.08 ms; DRG1, 3; RG1, 10 db; NS, 4; NECH, 6000; TE, 1.5 ms; DR, 2; and PRG, 1 (Zhou et al., 2023).

After the freeze-dried sample was fractured with liquid nitrogen and sprayed with gold, the microstructure of the intersecting surface was observed via SEM (SU 8020, Hitachi, Japan) at 30 kV to obtain the microstructures of samples (Li, Rao, et al., 2021).

2.4. Influence of different freeze-dried fruit powders on the 3D printing effect of gummy candy gels

2.4.1. Preparation of gummy candy gels

A high fructose corn mixture (10 g) was added to 30 mL of ultrapure water at 80 °C. After full dissolution, three grams PGP and five grams GE was added with magnetically stirring 40 min at 60 °C, five typical fruit powders that can basically achieve 3D printing with good taste and flavor were selected through pre-experiments to add in the gummy candy gels. Five grams and ten grams freeze-dried powder of strawberries, mulberries, mangoes, peaches, sea buckthorn were added in composite gel respectively with stirring 10 min to prepare low dose and high dose fruit powder source gummy candy gels. The composite gel without fruit freeze-dried powder was PGP/GE group.

2.4.2. Physical and chemical index testing of freeze-dried fruit powder

The total pectin content was determined via a total pectin content detection kit, and the results are represented on a dry basis (mg/g). The determination of dietary fiber content was performed according to the method of AOAC 985.29. pH measurement were performed using a pH meter. The total acid content was determined according to previous methods (Sedjoah et al., 2021), and the total acid content was expressed

as mg/g of lactate.

The DPPH clearance rate was determined according to previous methods (Sharma & Bhat, 2009). 1 mg freeze-dried fruit powder was dispersed in 10 mL of ultrapure water to prepare an extraction solution, which was then stirred. An equal amount of each freeze-dried powder was mixed with a DPPH ethanol solution and allowed to react at 25 °C for 30 min in the dark. Spectrophotometric measurements were performed at 517 nm. The data are presented as the means ± SD. The inhibition was calculated via Eq. (2):

$$\text{Inhibition}(\%) = \frac{A_0 - (A_1 - A_2)}{A_0} \quad (2)$$

Control group (A_0): 100 μL of DPPH solution and 100 μL of ethanol solution.

Sample group (A_1): 100 μL of extraction solution and 100 μL of DPPH ethanol solution.

Blank group (A_2): 100 μL of sample solution and 100 μL of ethanol solution.

The ABTS clearance rate was determined according to previous methods (Zulueta et al., 2009). Potassium persulfate solution (2.45 mmol/L) and ABTS solution (7 mmol/L) were mixed at a 1:1 ratio, and reacted at 25 °C for 12–16 h in the dark. The mother liquor was diluted to an absorbance of 0.70–0.72 at 734 nm with PBS. 1 mg of sample mixture was dissolved in 10 mL of distilled water to prepare the extraction solution. Then, 30 μL of sample solution was mixed with 170 μL of ABTS solution in a 96-well plate to react at 25 °C for 6 min in the dark. Spectrophotometric measurements were performed at 734 nm via an enzyme-linked immunosorbent assay (ELISA).

$$\text{Inhibition}(\%) = \frac{1 - (A_1 - A_2)}{A_0} \quad (3)$$

Control group (A_0): 200 μL of ABTS.

Sample group (A_1): 30 μL of sample solution and 170 μL of ABTS.

Blank group (A_2): 30 μL of sample mixture and 170 μL of PBS.

2.4.3. LF-NMR analysis

The determination method was the LF-NMR method described in Section 2.3.4.

2.4.4. 3D printing

The gel solutions prepared in 2.4.1 were used for 3D printing. A hexagonal star body (length of 60 mm, width of 60 mm, height of 15 mm) was used to evaluate the printability and 3D printing accuracy of the composite gel. The temperature remained at 30 °C. For other 3D printing parameters and printing accuracy calculation formulas, refer to the 3D printing process in Section 2.3.3.

2.4.5. Rheological measurements

The rheological measurements were performed according to the methods in Section 2.3.2.

2.4.6. Texture profile analysis

The texture properties of the gummy candy gels were detected via a texture analyzer (StableMicro System, Godalming, UK). The samples were cut into square shapes with dimensions of 1.5 × 1.5 cm. The parameters were as follows: the pretest speed was 5 mm/s, the test speed was 2 mm/s, the posttest speed was 2 mm/s, the compression strain was 50 % and the trigger force was 5 N (Meng et al., 2022).

2.4.7. Sensory evaluation of gummy candy gels

Ten food processing and safety graduate students with sensory evaluation experience were selected to conduct sensory evaluations for the study, scoring the color, elasticity, appearance, texture, and flavor of gummy candy gels. The average score of 10 people was used as the sensory evaluation score. The sensory scoring weight distributions and evaluation items were shown in Table S1.

2.5. Statistical analysis

The results were presented as the means ± standard deviations. The data were analyzed with SPSS software (Version 26.0, IBM Corporation, Somers, NY, USA) via one-way ANOVA, and differences among the data were considered to be significant ($p < 0.05$) according to the Duncan test.

3. Results and discussion

3.1. Selection of 3D-printed substrate composite gel

3.1.1. Rheological characteristics of the composite gels

The rheological characteristics of materials play an important role in determining printing performance and self-supporting capabilities in the process of 3D printing, which are closely related to the dynamic viscoelasticity and shear-thinning properties (Zhang et al., 2022). As shown in Fig. 1A, the viscosity of the composite gels decreased significantly as the shear rate increased from 0.1 s^{-1} to 100 s^{-1}, which indicated that the composite gels exhibited pseudoplasticity and shear thinning behavior. This behavior may be attributed to the shear stress reducing the number of entanglement nodes，resulting in a significant reduction in viscosity (Wei et al., 2019). The ideal food 3D printing material should have an appropriate viscosity, which can not only be easily extruded through the nozzle, but also be smoothly bonded with the previously deposited printed layer, and it must not deform after printing. PGP/GG and PGP/KC were difficult to extrude via 3D printing because of their relatively high apparent viscosities. PGP/GE was easy to extrude because of its lower apparent viscosity.

As shown in Fig. 1B，G′ was greater than G″ as the shear strain increased from 0.01 % to 1 %, indicating that the elasticity of the composite gel was greater than the viscosity. The G′ and G″ curves show a parallel trend within a certain strain range. This platform region is called the LVER. At 0.5 % strain, the G′ and G″ values of the composite gels were not related to the strain amplitude, so subsequent experiments were conducted at a strain value of 0.5 %. As shown in Fig. 1C and D, frequency scanning revealed that the G′ values of PGP/GG and PGP/KC were much greater than that of G″, which indicated that the solid-like properties of the samples were too strong. PGP/GG and PGP/KC were not suitable for the extrusion process of 3D printing，as it involved tow breakage and has poor printing quality. The difference between G′ and G″ of PGP/GE was not large, indicating that the elastic and viscous properties are relatively balanced.

Fig. 1E and F show that the G′ and G″ of the PGP/GG did not change significantly as the temperature changed, indicating that the viscosity of the sample changed little as the temperature changed, so it was not suitable for 3D printing. Simultaneously, G' and G" of the PGP /KC changed quickly because of their sensitivity to temperature, which was not conducive to controlling the temperature during the 3D printing process. When the loss factor is less than 1, it can be proved that the gel solution is a solid with poor fluidity, but this is more conducive to extrusion molding. If the loss factor is greater than 1, this may indicate that the solution is more fluid and flows easier (Wang et al., 2021). However, extrusion lines are easy to fuse because of the excessive fluidity of the liquid, which is not beneficial for 3D printability and formability. Fig.1G and 1H show that the loss factor of the PGP/GE composite gel was always less than 1, which indicated that the sample presented solid-like properties and was easy to 3D print. The loss factor of the PGP/KC group was greater than 1 as the temperature increases, and the fluidity of the sample was too strong to be conducive for 3D printing.

In conclusion, PGP/GE was easy to extrude because of its apparent viscosity lower than PGP/GG and PGP/KC. The elastic and viscous properties of PGP/GE are relatively balanced, while the solid-like properties of the PGP/GG and PGP/KC were too strong. These rheological results revealed that the PGP/GE composite gel was more

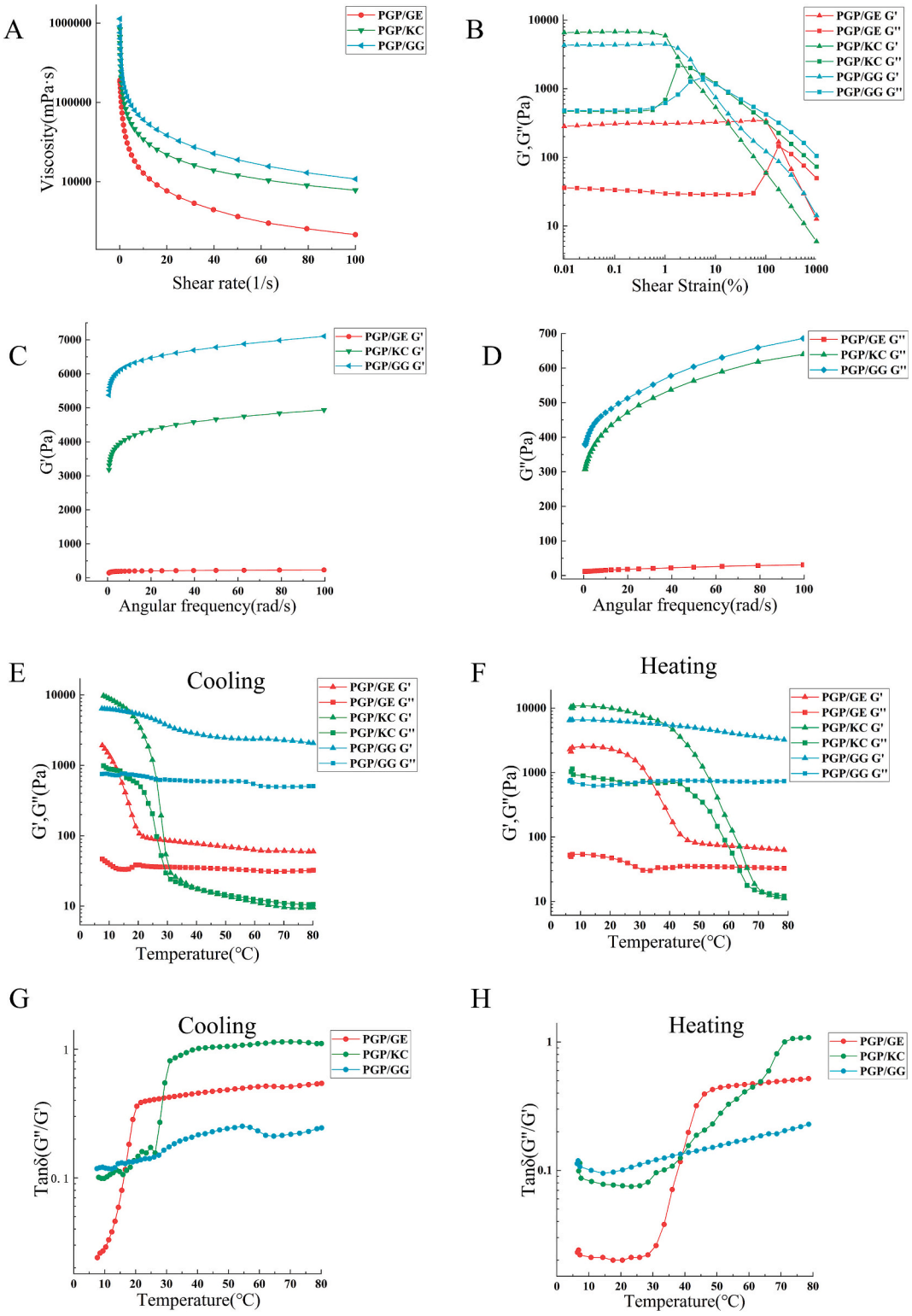

Fig. 1. Viscosity vs. The the shear rates of the composite gels(A). Shear strain sweep vs. the shear strain of the composite gels(B). Storage modulus G′ (C) and loss modulus G″ (D) vs. the angular frequency of the composite gels. The G′ and G″ curves of composite gels during the cooling process (E) and heating process (F) were obtained in temperature scanning mode. The tan δ (G″/G′) of the composite gels during the cooling process (G) and heating process (H).

suitable for 3D printing.

3.1.2. *3D printing accuracy of the composite gel*

The printing effects of the three different composite gels were shown in Fig. 2B. The PGP/GE had the best printing quality. The micelles of PGP/GG and PGP/KC fractured several times during 3D printing. The product surface was rough, which was consistent with the results of the rheological properties. This is likely because of the strong gel performance of the κ-carrageenan gel, and the viscosity value changes too quickly as the temperature changes. It is difficult to eliminate the small bubbles generated in the mixing process during the printing process because the PGP/KC has high hardness but poor ductility. PGP/GG has

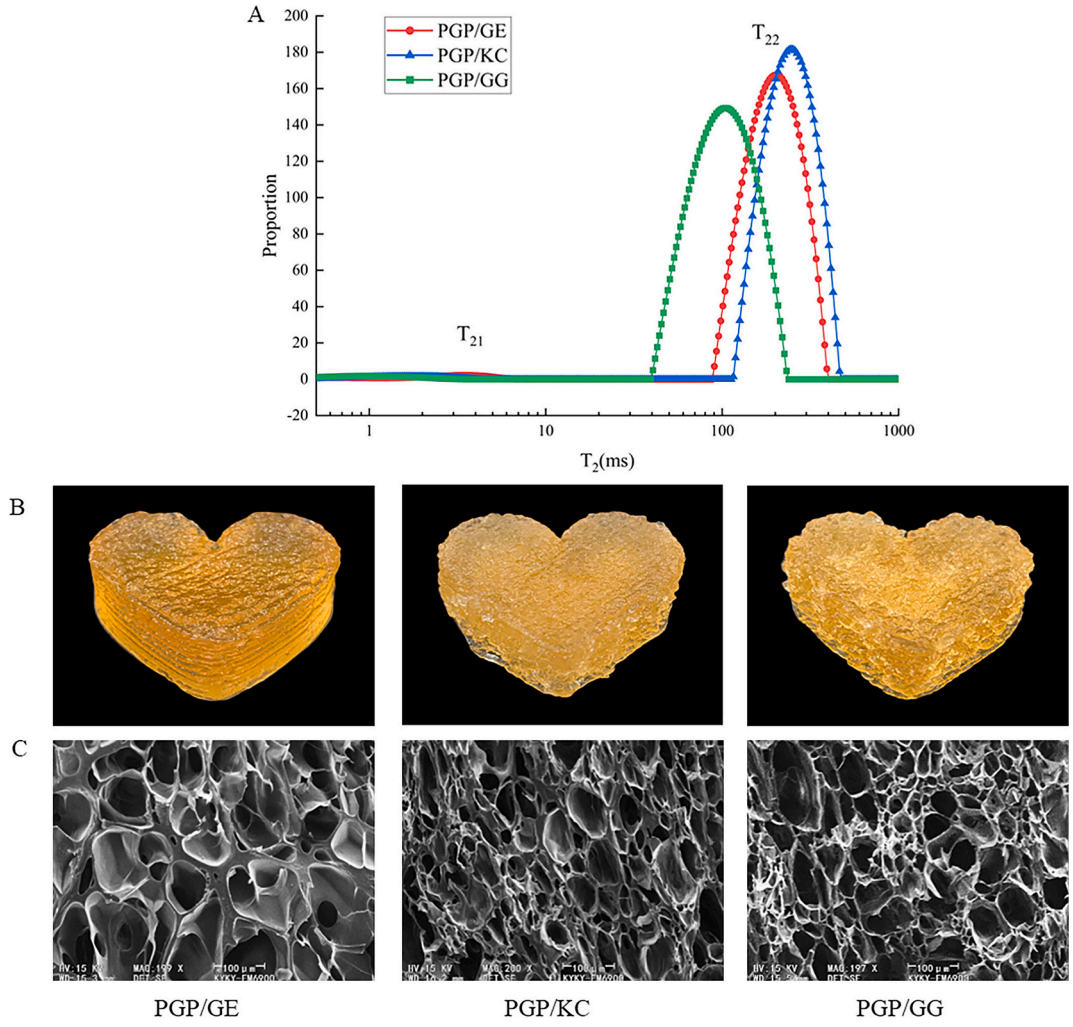

Fig. 2. Water state distribution (A), appearance of 3D-printed composite gels(B) and SEM image of the composite gels (C).

high viscosity during 3D printing, resulting in poor printing and severe line breaking, and the product surface is rough. The printing accuracy is close to 100 %, indicating that its water retention ability is better (Fan et al., 2020). As shown in Table S2, the printing accuracy of PGP/GE was greater than that of PGP/KC and PGP/GG ($P < 0.05$), and the printing accuracy in terms of the length and height of the samples was greater than 96 % after 3 h. Gellan gum destroyed the network structure and improved the hardness of the product by self-cooling cross-linking, which was based on the temperature-sensitive phase-change characteristics (Yan et al., 2022). The hardness of the PGP/GG composite gel was too high for extrusion at the printing temperature. The relatively high viscosity could lead to poor surface smoothness of PGP/KC and PGP/GG, and there could be difficulties in extrusion, bubble removal, and tow continuity. In this study, the PGP/GE group had the best 3D printing performance.

3.1.3. LF-NMR and SEM of the composite gels

As shown in Fig. 2A, T_{21} represents combined water in the macromolecular structure, and T_{22} represents free water outside the network structure. The water distribution of a composite gel affects its 3D printability. The combined water promotes the printability of the gel, whereas the free water is conducive to the fluidity of the gel in the printing process (Li et al., 2023). The T_{22} relaxation time of PGP/GG was shorter than that of PGP/GE and PGP/KC, possibly because PGP/GG attracted water molecules through hydrogen bonds or hydrophobic bonds during the formation of the gel, and its gel network had a strong ability to bind water molecules and reduce the movement of water molecules (Yan et al., 2022). The results indicated that the PGP/GG composite gel formed a denser network structure, stronger plasticity and less fluidity than the other two composite gels did. Therefore, the extrusion and printing properties of PGP/GE and PGP/KC were better than PGP/GG during 3D printing.

Fig. 2C shows that the micropores in the PGP/KC and PGP/GG groups were less uniform and greater in pore size than those in the PGP/GE group. The pore distribution of the microstructure affects the extrudability and surface structure of products (Liu et al., 2018). This is probably due to the formation of a pronounced gel-like matrix, which endows 3D printing ink with mechanical stability, increasing the cross-linking density of hydrogels through increased hydrogel strength and the mechanical strength of the inks (Pant et al., 2021). However, if the mechanical strength is too high in the printing process, it will easily lead to line fracture and extrusion difficulties. PGP/KC and PGP/GG presented crosslinked and porous structures, and the pore distribution was uneven. This may be due to excessive mechanical strength, line breaking, and poor line fusion during extrusion, resulting in defects in the printed sample.

The PGP/GE had the lowest apparent viscosity among the three kinds of composite gels, and had moderate extrusion properties and the best 3D printing quality. The rheological results are in accordance with the 3D printing results. Furthermore, microstructure analysis revealed that PGP/GE formed a relatively loose and uniform gel structure and endowed the gel with good water retention and self-supporting ability.

Therefore, the PGP/GE composite gel was selected as the substrate material for subsequent 3D printing experiments of fruit powder gel.

3.2. Effects of different freeze-dried fruit powder on the 3D printing of gummy candy gels

3.2.1. Physicochemical indicators of freeze-dried fruit powder

The physical and chemical indicators of yellow peach, strawberry, mulberry, mango and sea buckthorn freeze-dried powders are shown in Fig. 3. Pectin is a lipophilic colloid and an anionic polyelectrolyte. It is widely used as a gelling agent and stabilizer in the food industry (Wedamulla et al., 2023b). Therefore, the content and type of pectin in lyophilized fruit powder strongly influence the properties of gels. For example, Gallery et al. (2024) reported that citrus-based pectins presented greater rheological performances than apple-based pectins. This suggests that the deformability of the gels is driven by the methyl ester groups, whereas the hardness of the gels is driven more by the amide groups. However, the gel strength of amidated low-methoxyl pectins is driven more by the amidation. Through the formation of numerous hydrogen bonds between the amide groups, the stabilization of the junction zones of the network structure of the amidated low-methoxy gels was promoted, resulting in strengthened gels. The vitamin E microcapsules were encapsulated with the gelatin high-methoxyl-pectin (GA-HMP) and gelatin low-methoxyl-pectin (GA-LMP) complex coacervates (Zhou et al., 2024). More aggregates and denser networks formed at a gelatin-pectin ratios of 3:1 and pH of 4.0, and GA-HMP had better thermal stability than GA-LMP did. The pH value is an important parameter in complex gel systems, and its change affects the surface charge distribution of starch and polysaccharides, affecting the attraction and repulsion between proteins and polysaccharide gels (Gao et al., 2023), A high pH value may lead to hydrolysis of peptide chains in gelatin molecules, damaging the molecular structure of gelatin and reducing the gel strength. In addition, dietary fiber is one of the major influencing factors. Nie et al. (2024) reported that IDF and SDF can improve the gelation of surimi and that the gel properties of surimi increase and then decrease as the SDF content increases. The gel strength, deformation resistance and elasticity of surimi increased with increasing IDF content, but its effect on viscosity and recovery ratio was similar to that of SDF. Cheng et al. (2024) studied the effects of IDF on the 3D printing characteristics and molecular interactions of wheat gluten and soy protein isolates. When the IDF increased from 0 to 10 %, 3D-printed plant-based meats presented improved water retention, elongation at break, and tensile strength, which demonstrated excellent printing performance. The proportion of IDF and SDF in strawberry powder is relatively high, and the effect of 3D printing of its composite gel may be better.

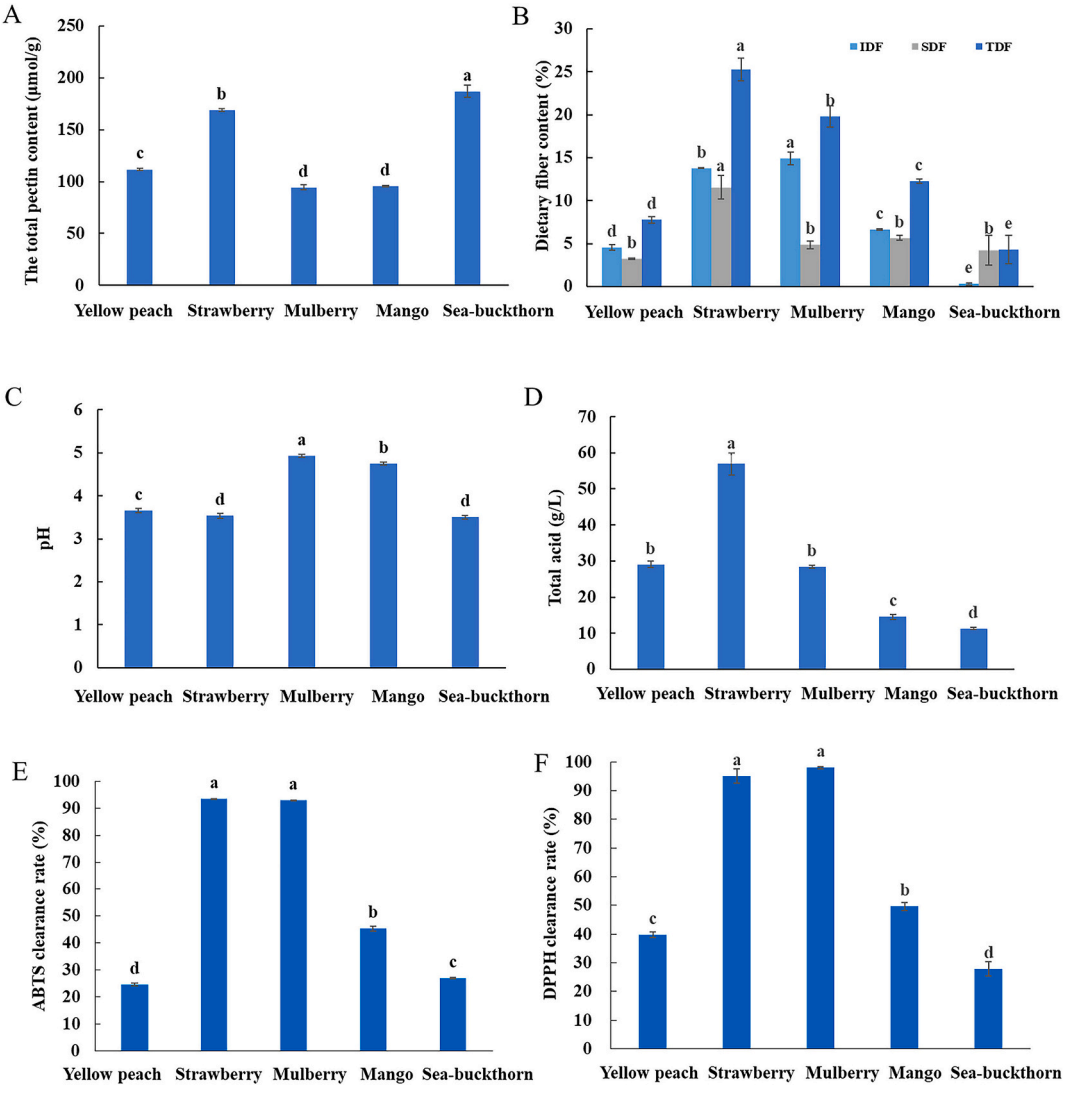

Fig. 3. Physical and chemical indicators of freeze-dried powders from different fruits.

3.2.2. LF-NMR analysis of gummy candy gels

The water distribution of food in ingredients is strongly related to their physical properties. As shown in Fig. 4 and Table S3, the T_{22} of the PGP/GE group was greater than that of the other two groups, indicating that the combined ability of water and solids in the composite gels without freeze-dried fruit powder was weaker than that of the sample with freeze-dried fruit powder. Compared with that of the PGP/GE group, the transverse relaxation time of the freeze-dried fruit powder composite gels shifted significantly to the left. This may be because the pectin in the freeze-dried fruit powder limited the movement of water molecules in the gel. The free water in the composite gel gradually transferred to the bound water with increasing amounts of freeze-dried fruit powder. There are hydrophilic polysaccharides in fruit powder, such as pectin, which can bind to multiple water molecules through hydroxyl and carboxyl structures. The proper addition of freeze-dried fruit powder could improve the interaction between the gel and water molecules to allow the gel network to incorporate more water (Yu et al., 2024). As shown in Fig. 3A, the pectin content of strawberry powder was highest among the five kinds of fruits, which is consistent with the fact that the free water content of the strawberry powder decreased the most. The high free water content of sea buckthorn resulted in the weak water binding ability of its composite gel. This phenomenon is related to the pectin type, low dietary fiber content, and low acid conditions of sea buckthorn, which may also affect the ability of its pectin and dietary fiber to bind to water solids. In summary, the gummy candy gels with strawberries and mangoes freeze-dried powder, especially with strawberries, exhibited strong water retention abilities.

3.2.3. Effects of the addition of freeze-dried fruit powder on the 3D printing accuracy of gummy candy gels

Fig. 5 shows the 3D printing appearance of composite gels from different freeze-dried fruit powders. There was a collapse phenomenon in the mulberry group, whereas poor printing quality was observed in the sea buckthorn group. Because the gel network and chain density were weak, the extrusion lines were easy to fuse, and the support was insufficient, so the preset effect could not be achieved. The printing effect of sea buckthorn and mulberry gel in the high-dose group was worse than that in the low-dose group. The 3D printing effect of the low-dose yellow peach, strawberry and mango groups was slightly better than that of the high-dose group. Table S4 shows the printing accuracy of the composite gels from different freeze-dried fruit powders stored at 25 °C for 0–3 h. The printing accuracy slightly changed with the addition of low-dose fruit powder. As the addition of fruit powder increased, the printing accuracy decreased significantly after 3 h. This may have occurred because the total acid content increased with the addition of the freeze-dried fruit powder, and the instability of the gel at higher acid contents might have led to the release of some water from the pectin-water-sugar network (Makroo et al., 2019). In addition, this may have been because of the increase in dietary fiber content. Ouyang et al. (2024) reported that the quality of bread and increased hardness and moisture loss during storage are reduced when too much soluble dietary fiber (12 %) or insoluble dietary (>8 %) is added. Therefore, proper addition of strawberry, yellow peach and mango powder could improve the appearance of 3D printing.

3.2.4. Effects of the addition of freeze-dried fruit powder on the rheological characteristics of gummy candy gels

The apparent viscosity (η) values of all the freeze-dried fruit powder gels decreased with increasing shear rate, indicating shear thinning (Liu, Bhandari, et al., 2019). The structure of the freeze-dried fruit powder gel was relatively stable under the action of pectin at low shear rates. The interaction between molecules weakened as the shear rate increased, resulting in a reduction in the flow resistance and η value. The η value of the composite gel increased with increasing fruit powder doses, except in the sea buckthorn group. Fig. 6A shows the viscosity of different fruit powder composite gels at a printing temperature of 30 °C, which was yellow peach>mango>strawberry>mulberry and sea buckthorn. The higher the η value is, the greater the viscosity of the gel. In 3D printing, a specific viscosity is required to support the layer-by-layer deposition of ink materials. Therefore, the viscosity of the ink cannot be too low. As shown in Fig. 3B, the content of SDF in mulberry was low, whereas the proportion of IDF in mulberry was relatively high. The composition of dietary fiber may be one of the reasons for the low viscosity of mulberry composite gel. Compared with IDF, SDF generally has a greater viscosity and gel ability (Dong et al., 2022). The contents of IDF and SDF in sea buckthorn were low, and the shear thinning phenomenon of the system was further enhanced, which can be explained by the reduction in molecular entanglement caused by the shear process, resulting in a decrease in viscosity (Zhang et al., 2024). Combined with the LF-NMR analysis results, the free water content of sea buckthorn was high, indicating that the ability of the composite gel to combine with water was relatively weak after adding sea buckthorn fruit powder, which further affected the viscosity of the composite gel of sea buckthorn. The structural characteristics of pectin from different fruits are very different because of different varieties, which leads to differences in gel properties (Cui et al., 2023). The compact conformation of pectin contributes to the formation of hydrophobic forces and hydrogen bonds near molecules, resulting in the formation of a stable three-dimensional network. When pectin is dissolved in water with weak acid to neutral pH, the carboxyl groups on the galacturonic moiety dissociate and generate negative charges, resulting in repulsive forces between adjacent pectin molecules and between pectin and water, which prevents pectin molecules from forming gels. When the pH decreased to less than 3.5, the repulsive forces decreased to a negligible value (Ganatra et al., 2024). Fig. 3A, C and D shows that the pectin content and total acid content of strawberry and yellow peach are high, and the pH is low, which contributes to

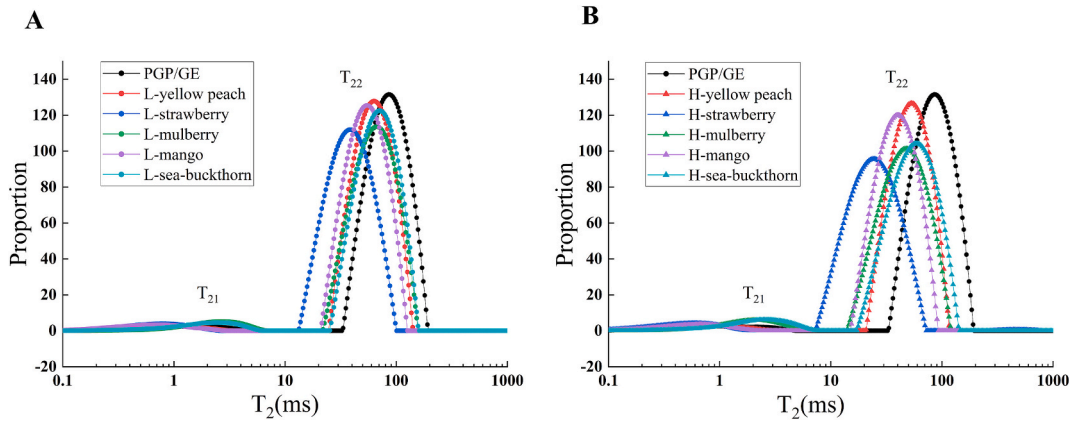

Fig. 4. Water state distribution of the gummy candy gels.

Fig. 5. 3D printing appearance of different freeze-dried fruit powder composite gels at low doses (A) and high doses (B).

reducing the repulsion force between pectin molecules and the formation of a gel. In addition, although the dietary fiber content of mango is not high, but the gel properties are good, which may be due to the appropriate proportion and additive amount of SDF and IDF because an appropriate additive amount of SDF and IDF can enhance the network structure of the gel and improve its deformation resistance (Nie et al., 2024). In conclusion, the viscosity values of yellow peach, strawberry and mango composite gels were relatively high, which could provide better support in the printing process and is conducive to 3D printing.

Fig. 6B and C shows that the intersection of the G′ and G″ curves is the minimum flow stress point (τf point), which indicates the minimum stress required for the composite gel to start flowing (Jiang et al., 2019). The minimum flow stress can be used to judge the difficulty of printing material extrusion through the piston (Zhu et al., 2019). The smaller the τf value is, the easier the material is extruded (Liu, Yu, et al., 2019). The minimum flow stress values of gels from different freeze-dried fruit powders were as follows: mango>yellow peach>strawberry>mulberry>sea buckthorn. The τf values of the yellow peach, mango and strawberry groups increased with increasing fruit powder doses, but the τf values of the mulberry and sea buckthorn groups decreased with increasing fruit powder doses, which was related to the G′ value of the fruit powder gel. The addition of yellow peach, mango and strawberry powder increased the mechanical strength of the gel, which could improve the shape maintenance rate after extrusion, whereas the addition of mulberry and sea buckthorn powder decreased the mechanical strength of the gel, and the extrusion process was difficult to control.

As shown in Fig. 6D and E, the G′ and G″ values of the fruit powder gels were dependent on the oscillation frequency; with increasing angular frequency, the G′ and G″ values also increased. The results revealed that the G′ value of the composite gel with a low dose of fruit powder was as follows: yellow peach>mango>strawberry>mulberry>sea buckthorn, and the G″ value was as follows: yellow peach>strawberry>mango, mulberry>sea buckthorn. The G′ and G″ values of the composite gel with a high dose of fruit powder were strawberry>yellow peach>mango>mulberry>sea buckthorn. Materials with higher G′ and G″ values have greater mechanical strength to maintain the stability of the printing structure (Alvarez et al., 2009). Except for the sea buckthorn group, the G′ and G″ values of the other four kinds of fruit powder gels increased significantly after the dose increased. This result indicated that the mechanical strength of the gel increased with increasing fruit powder content. The G′ values of fruit powder gels are always greater than the G″ values, and tanδ is less than one, which indicates that the gel is in a solid-like state (Yang et al., 2019). The G′ and G″ values of strawberry, yellow peach and mango gels were always greater than those of mulberry and sea buckthorn gels, which was related to the type and proportion of pectin and dietary fiber in each. Under acidic conditions, gummy candy gels form noncovalent bonds to form entangled networks. This phenomenon has been reported in pectin gels, whose polymer gels are easily entangled in acidic environments and high solute concentrations (Liu, Yu, et al., 2019). Therefore, combined with 3D printing results, these oscillation frequency results revealed the addition of strawberry, yellow peach and mango powder can maintain good shape fidelity of gels after printing.

As shown in Fig. 7A, B, C, and D, under dynamic temperature scanning, after increasing the dose of fruit powder, the G′ and G″ values of the high-dose fruit powder group were greater than those of the low-dose group, with the exception of the sea buckthorn group. The G′ values of yellow peach and mango were greater than those of the other fruit powder groups at relatively low temperatures. With increasing temperature, the range of G′ values of strawberry fruit powder gradually decreased, and the temperature increased. The G' of strawberry fruit powder was greater than that of yellow peach and mango fruit powders, indicating that the effect of temperature on the G′ of strawberry fruit powder was smaller than that on mango and yellow peach fruit powders. This may be due to the high pectin content and dietary fiber content of strawberry fruit powder, resulting in its strong ability to bind water, produce high viscosity and strengthen network structure. Strawberry fruit powder has a strong ability to combine with water, resulting in less free water. Under high temperature, the G′ of the strawberry group was greater than that of the yellow peach group and mango group as the temperature decreased. Wedamulla et al. (2023a) reported that the addition of pectin increased the 3D printability, viscosity and G′ of a gel at relatively high temperatures (80 °C and 90 °C). Cheng et al. (2024) reported that there is a higher number of hydrogen bonds, hydrophobic bonds, and disulfide bonds between IDF and protein, resulting in the formation of more stable structures and improved 3D printing molding performance within a certain concentration range. The LF-NMR results also verified the strong water binding ability of the strawberry composite gel. Therefore, the rheological behavior of strawberry samples was more suitable for 3D printing at relatively high temperature. The rheological behavior of yellow peach and mango samples was more conducive to 3D printing at relatively low temperature. Sea buckthorn and mulberry samples showed poor rheological behavior under temperature scan, which was not suitable for 3D printing.

3.2.5. Texture profile analysis of gummy candy gels from different freeze-dried fruit powders

The texture profiles of different freeze-dried fruit powder gummy candy gels were tested as shown in Table 1. The springiness, cohesiveness, and resilience of gummy candy gels from different freeze-dried fruit powders were not significantly different ($p < 0.05$). Under the

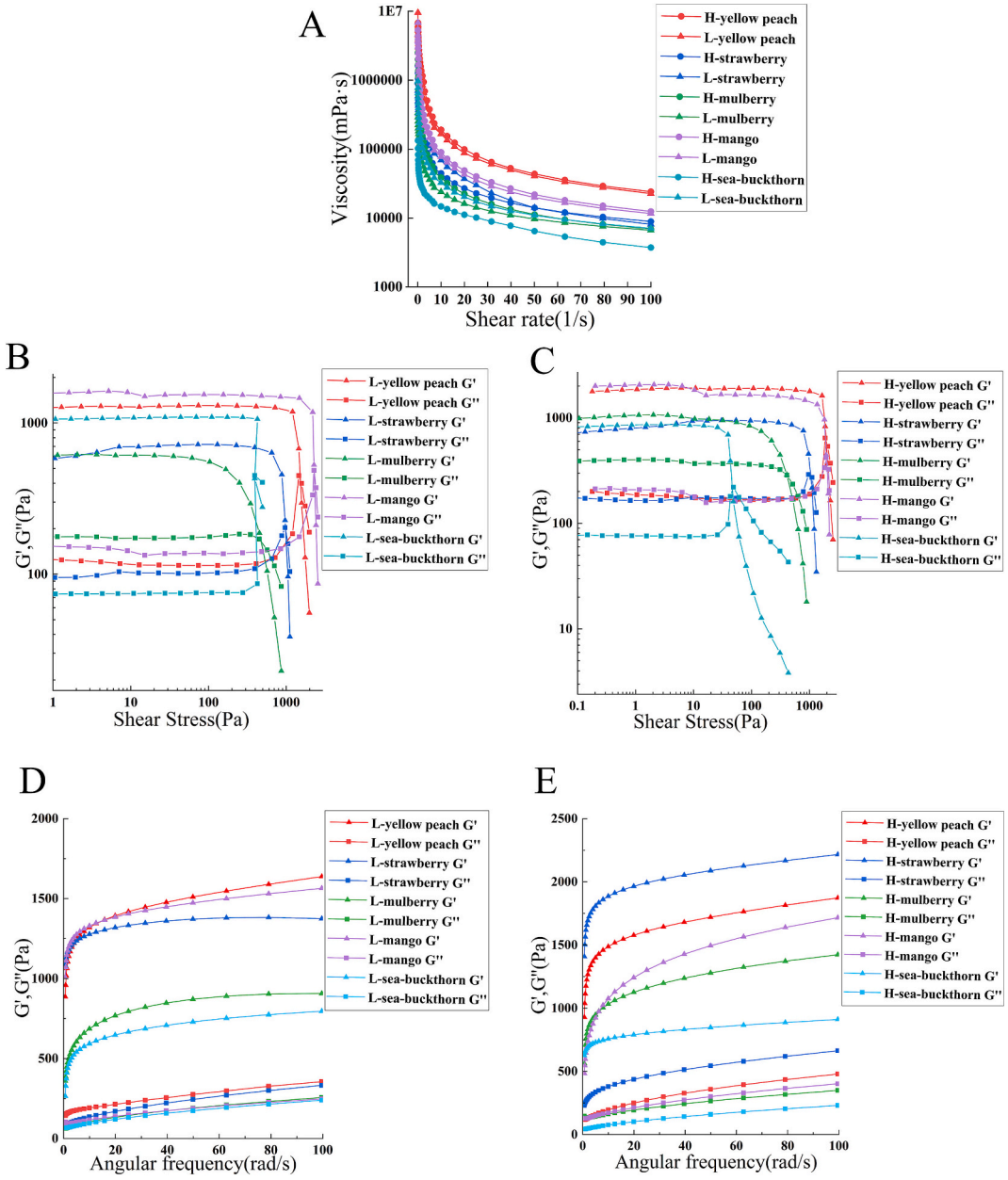

Fig. 6. Dependence of viscosity on shear rate from 0.1 s^{-1} to 100 s^{-1} for gummy candy gels (A). Shear strain sweep of low-dose (B) and high-dose (C) gummy candy gels. Dependence of G′ and G″ on the angular frequency of gummy candy gels at low doses (D) and high doses (E).

condition of a low dose of freeze-dried fruit powder, the hardness of gummy candy gels with different fruit powders was ranked as follows: strawberry>yellow peach>mango>mulberry>sea buckthorn. The high hardness value of the strawberry group is likely because the content of dietary fiber in freeze-dried strawberry powder has a greater effect on gel properties, and the strong binding ability between dietary fiber and free water leads to a decrease in free water, thus increasing gel hardness. The high hardness value of the yellow peach sample may be related to its high pectin content and appropriate dietary fiber ratio, which results in the formation of a more stable network structure gel with PGP. Furthermore, the increase in gel hardness may also be due to the formation of hydrogen bonds between pectin and hydrocolloids under acidic conditions, which strengthens the gel structure (Ganatra et al., 2024). The hardness value of the low-dose sea buckthorn gummy candy gels was greater than that of the high-dose gels, which might be related to their low total acid content and high pectin content. With increasing addition of sea buckthorn fruit powder, a stronger repulsion force between pectin molecules and water molecules was generated under weakly acidic conditions, which led to difficulty in the formation of a gummy candy gel network and reduced the hardness of sea buckthorn gummy candy gels. The gumminess of gummy candy gels also showed a similar trend to that of hardness. LF-NMR analysis revealed that mulberry and sea buckthorn have a weak ability to bind water, indicating that they may contain more hydrophobic components, which might reduce the cohesiveness of the gel structure, resulting in a decrease in the gumminess value. The relatively low content of total acid affects the gelation of PGP and subsequently reduces the gumminess value of gummy candy gels. Chewiness is the energy required to make solid food ready for swallowing, which is determined by multiplying hardness, cohesiveness, and springiness (Tarahi et al., 2023). The degree of chewing of strawberry and yellow peach gummy candy gels was relatively high, which might be related to the relatively high total acid content, which reduces the pH value; makes PGP and pectin better able to form a gel network; and increases gel hardness, cohesiveness and

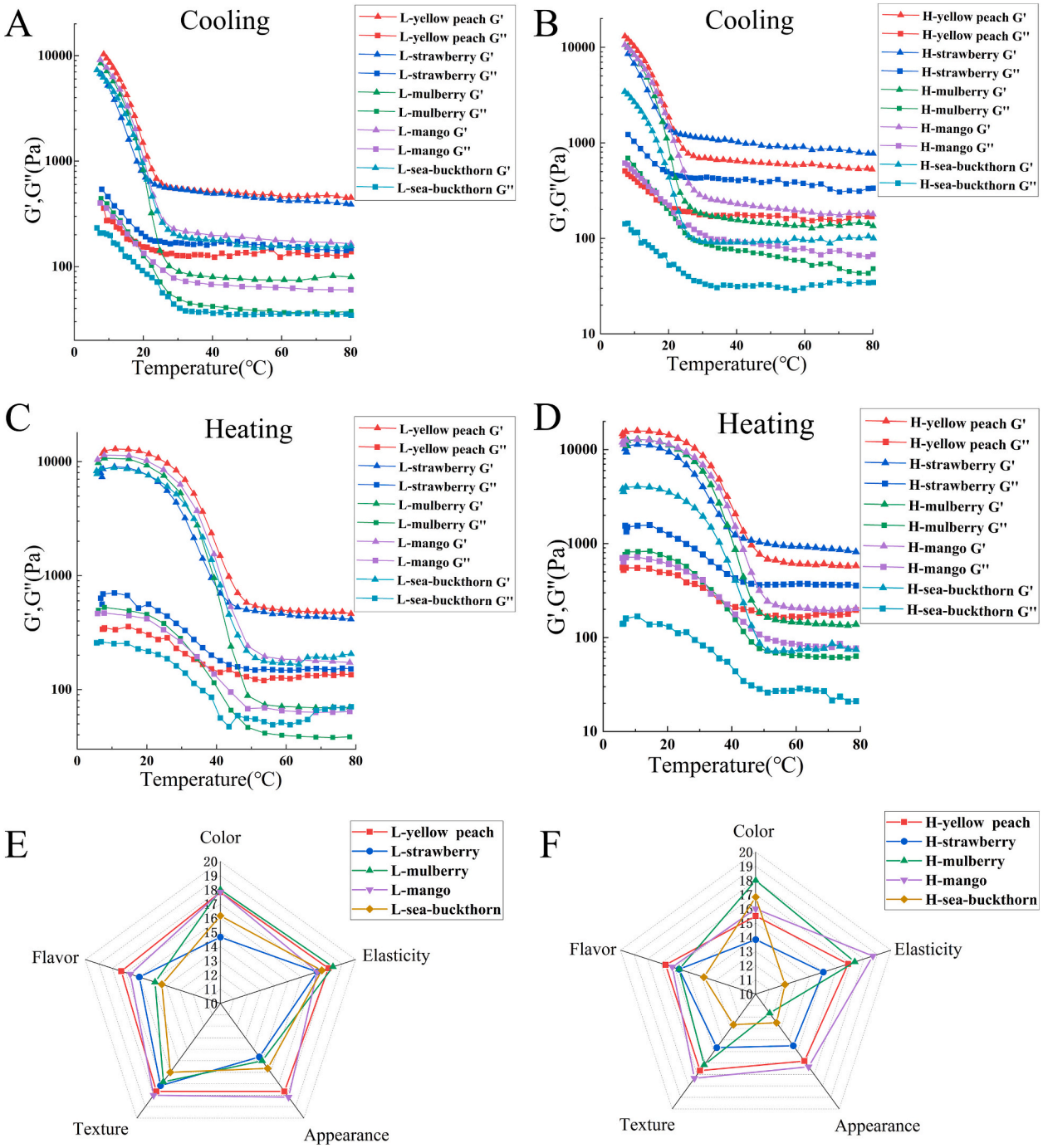

Fig. 7. G′ and G″ curves of gummy candy gels during the cooling process (A-B) and heating process (C—D) tested in temperature scanning mode. Sensory evaluation of different fruit powder gummy candy gels at low doses (E) and high doses (F).

springiness. Sea buckthorn may contain hydrophobic components such as sea buckthorn oil (Ganatra et al., 2024), and a low dietary fiber content, resulting in poor gelation of gummy candy gels and affecting chewiness. Therefore, the hardness and chewiness of the gummy candy adding strawberry, mango and yellow peach powder were better than that adding mulberry and sea buckthorn powder. Under the condition of a low dose of freeze-dried fruit powder, the hardness of gummy candy gels with strawberry>yellow peach>mango.

3.2.6. *Sensory evaluation of different fruit powder gummy candy gels*

As shown in Fig. 7E and F, the sensory evaluation results indicate that the sensory scores of the high-dose fruit powder group were lower than those of the low-dose fruit powder group. On the one hand, the increase in the amount of fruit powder led to changes in the texture profile of the product. On the other hand, the freeze-dried fruit powder contains organic acids, and a high dose of fruit powder leads to a sour taste in the product, which reduces overall acceptability. The sensory evaluation values of the high-dose sea buckthorn and strawberry groups decreased most significantly compared with those of the low-dose groups. The main reason for the decline in the sea buckthorn group was that the addition of high dose sea buckthorn powder led to a high content of free water in the product, and the product exhibited a water seepage phenomenon, which led to a reduction in texture characteristics and deterioration of taste. The reason why the score of the strawberry

Table 1
Texture profile of the gummy candy gels from different freeze-dried fruit powders.

Samples	Hardness (g)	Springiness (%)	Cohesiveness	Gumminess (N)	Chewiness(g)	Resilience –
L-yellow peach	2322.44 ± 6.767^{c}	0.98 ± 0.002^{a}	0.95 ± 0.004^{b}	2200.63 ± 14.57^{b}	2152.55 ± 18.564^{b}	0.65 ± 0.006^{bc}
L-strawberry	2682.94 ± 65.154^{g}	0.97 ± 0.008^{cd}	0.88 ± 0^{d}	2356.06 ± 55.689^{f}	2288.44 ± 36.112^{e}	0.58 ± 0.001^{e}
L-mulberry	1413.58 ± 36.959^{f}	0.95 ± 0.004^{a}	0.9 ± 0.006^{c}	1275.07 ± 42.312^{e}	1211.67 ± 44.44^{d}	0.62 ± 0.007^{cd}
L-mango	1811.53 ± 47.856^{b}	0.97 ± 0.006^{a}	0.96 ± 0.027^{d}	1733.16 ± 39.071^{b}	1680.26 ± 34.671^{b}	0.71 ± 0.034^{a}
L-sea buckthorn	1195.6 ± 47.094^{i}	0.94 ± 0.006^{a}	0.93 ± 0.015^{a}	1110.46 ± 35.01^{g}	1038.74 ± 36.997^{f}	0.63 ± 0.009^{a}
H-yellow peach	2707.13 ± 30.221^{a}	0.95 ± 0.003^{ab}	0.9 ± 0.009^{d}	2439.18 ± 21.423^{a}	2319.6 ± 27.564^{a}	0.76 ± 0.004^{d}
H-strawberry	2653.09 ± 39.373^{h}	0.95 ± 0.008^{bc}	0.92 ± 0.008^{e}	2434.1 ± 19.829^{g}	2321.98 ± 15.746^{f}	0.54 ± 0.004^{f}
H-mulberry	1699.97 ± 26.33^{d}	0.95 ± 0.014^{a}	0.93 ± 0.03^{d}	1586.55 ± 67.252^{c}	1511.34 ± 83.327^{c}	0.65 ± 0.017^{d}
H-mango	1836.1 ± 52.035^{e}	0.95 ± 0.001^{d}	0.88 ± 0.008^{d}	1624 ± 38.535^{d}	1545.84 ± 38.151^{d}	0.66 ± 0.008^{e}
H-sea buckthorn	747.51 ± 27.193^{j}	0.96 ± 0.001^{a}	0.98 ± 0.013^{ab}	730.88 ± 28.526^{h}	703.15 ± 26.599^{g}	0.65 ± 0.011^{b}

Values with different lowercase letters in the same column are significantly different ($P < 0.05$);

group decreased was that the total acid content of the strawberry powder was high. A high dose of strawberry powder led to high acidity, and the acid/sweet ratio was imbalanced, resulting in a hard taste and an inability to chew easily. The low-dose yellow peach and low-dose strawberry groups presented the highest comprehensive sensory scores with the best flavors and the highest overall acceptability. Considering that the strawberry group presented greater antioxidant ability, the 5 g (16.67 % w/v) strawberry gel group presented the best sensory evaluation in terms of sensory and nutritional value.

4. Conclusion

This study compared the 3D printing effects of gelatin, k-carrageenan, and gellan gum combined with a PGP composite gel. PGP/GE had good water retention and self-supporting ability. The results showed that the PGP/GE composite gel had the best 3D printing quality and stability. Therefore, the PGP/GE composite gel was selected for experiments with the fruit powders gel. When different freeze-dried fruit powders (strawberry, mulberry, mango, yellow peach, and sea buckthorn) were added to the PGP/GE composite gel, the addition of fruit powder increased the water retention performance of the composite gel, and the sensory quality of gummy candy gels with 5 g (16.67 % w/v) of fruit powder was better than that with 10 g (33.33 % w/v) of fruit powder. Compared with sea buckthorn and mulberry, yellow peach, strawberry and mango powder were more suitable as 3D printing ink. In combination with its printing performance, sensory quality and nutritional value, strawberry powder was better than yellow peach powder and mango powder. We can attempt to address the drawbacks of 3D printing of mulberry and sea buckthorn composite gels by adding hydrophilic substances (such as dietary fiber) or adjusting the acidity to enrich the materials of 3D printing fruits in the hope of preparing 3D printing fruit gel gummy candy gels with better performance and nutritional value.

CRediT authorship contribution statement

Ye-Xing Liang: Writing – original draft, Data curation. **Jing-Bing Xu:** Supervision. **Li Zhou:** Data curation. **Xue Li:** Supervision. **Ling Zhang:** Supervision. **Fan-Bing Meng:** Writing – original draft, Data curation.

Declaration of competing interest

The authors declare that they have no known competing financial interests or personal relationships that could have appeared to influence the work reported in this paper.

Acknowledgements

This research was supported by Research and Demonstration Promotion of Industrial Processing Technology for Chongqing Xiaomian, Sichuan Innovation Team of National Modern Agricultural Industry Technology System (SCCXTD-2024-26) and Sichuan Province Pilot Project for Deep Integration Reform of Industry and Education.

Appendix A. Supplementary data

Supplementary data to this article can be found online at https://doi.org/10.1016/j.fochx.2025.102464.

Data availability

No data was used for the research described in the article.

References

Abedinia, A., Ariffin, F., Huda, N., & Mohammadi Nafchi, A. (2017). Extraction and characterization of gelatin from the feet of Pekin duck (*Anas platyrhynchos domestica*) as affected by acid, alkaline, and enzyme pretreatment. *International Journal of Biological Macromolecules, 98*, 586–594. https://doi.org/10.1016/j.ijbiomac.2017.01.139

Alvarez, M. D., Fernández, C., & Canet, W. (2009). Enhancement of freezing stability in mashed potatoes by the incorporation of kappa-carrageenan and xanthan gum blends. *Journal of the Science of Food and Agriculture, 89*(12), 2115–2127. https://doi.org/10.1002/jsfa.3702

Azam, R. S. M., Zhang, M., Bhandari, B., & Yang, C. H. (2018). Effect of different gums on features of 3D printed object based on vitamin-D enriched orange concentrate. *Food Biophysics, 13*, 250–262. https://doi.org/10.1007/s11483-018-9531-x

Cheng, Z., Qiu, Y., Bian, M., He, Y., Xu, S., Li, Y., & Lyu, F. (2024). Effect of insoluble dietary fiber on printing properties and molecular interactions of 3D-printed soy protein isolate-wheat gluten plant-based meats. *International Journal of Biological Macromolecules, 258*, Article 128803. https://doi.org/10.1016/j.ijbiomac.2023.128803

Cui, J., Zhang, L., Wang, J., Zhao, S., Zhao, C., Liu, D., & Zheng, J. (2023). Study on the relationship between primary structure/ spatial conformation and gel properties of pectins from different varieties. *Food Hydrocolloids, 144*, Article 109055. https://doi.org/10.1016/j.foodhyd.2023.109055

Dong, R., Liao, W., Xie, J., Chen, Y., Peng, G., Xie, J., & Yu, Q. (2022). Enrichment of yogurt with carrot soluble dietary fiber prepared by three physical modified treatments: Microstructure, rheology and storage stability. *Innovative Food Science & Emerging Technologies, 75*, Article 102901. https://doi.org/10.1016/j.ifset.2021.102901

Fan, H., Zhang, M., Liu, Z., & Ye, Y. (2020). Effect of microwave-salt synergetic pretreatment on the 3D printing performance of SPI-strawberry ink system. *LWT, 122*, Article 109004. https://doi.org/10.1016/j.lwt.2019.109004

Gallery, C., Agoda-Tandjawa, G., Bekaert, D., & Gitto, L. (2024). Understanding structure/rheology relationships of amidated low-methoxyl citrus and apple pectin gels: Implications of sucrose, pectin types and characteristics. *Food Hydrocolloids, 152*, Article 109950. https://doi.org/10.1016/j.foodhyd.2024.109950

Ganatra, P., Jyothish, L., Mahankal, V., Sawant, T., Dandekar, P., & Jain, R. (2024). Drug-loaded vegan gummies for personalized dosing of simethicone: A feasibility study of semi-solid extrusion-based 3D printing of pectin-based low-calorie drug gummies. *International Journal of Pharmaceutics, 651*, Article 123777. https://doi.org/10.1016/j.ijpharm.2024.123777

Gao, R., Song, R., Shen, L., Zhao, X., Xue, L., Li, J., & Zheng, X. (2023). Evaluation of 3D printability of blueberry powder gel system under ultrasound pretreatment. *LWT, 190*, Article 115577. https://doi.org/10.1016/j.lwt.2023.115577

Jiang, H., Zheng, L., Zou, Y., Tong, Z., Han, S., & Wang, S. (2019). 3D food printing: Main components selection by considering rheological properties. *Critical Reviews in Food Science and Nutrition, 59*(14), 2335–2347. https://doi.org/10.1080/10408398.2018.1514363

Jiang, Q. Y., Zhang, M., & Mujumdar, A. S. (2022). Novel evaluation technology for the demand characteristics of 3D food printing materials: A review. *Critical Reviews in Food Science and Nutrition, 62*(17), 4669–4683. https://doi.org/10.1080/10408398.2021.1878099

Li, Q. H., Li, S. Y., Yu, W. K., Xiao, J. X., & Huang, G. Q. (2023). Comparison of the 3D printability of high internal phase Pickering emulsions stabilized by protein-polysaccharide complexes and process optimization. *Journal of Food Engineering, 353*, Article 111548. https://doi.org/10.1016/j.jfoodeng.2023.111548

Li, Y.-C., Du, W., Meng, F.-B., Rao, J.-W., Liu, D.-Y., & Peng, L.-X. (2021). Tartary buckwheat protein hydrolysates enhance the salt tolerance of the soy sauce fermentation yeast *Zygosaccharomyces rouxii*. *Food Chemistry, 342*, Article 128382. https://doi.org/10.1016/j.foodchem.2020.128382

Li, Y. C., Rao, J. W., Meng, F. B., Wang, Z. W., Liu, D. Y., & Yu, H. (2021). Combination of mutagenesis and adaptive evolution to engineer salt-tolerant and aroma-producing yeast for soy sauce fermentation. *Journal of the Science of Food and Agriculture, 101*(10), 4288–4297. https://doi.org/10.1002/jsfa.11068

Licá, I. C. L., Soares, A. M. D. S., De Mesquita, L. S. S., & Malik, S. (2018). Biological properties and pharmacological potential of plant exudates. *Food Research International, 105*, 1039–1053. https://doi.org/10.1016/j.foodres.2017.11.051

Liu, Y., Yu, Y., Liu, C., Regenstein, J. M., Liu, X., & Zhou, P. (2019). Rheological and mechanical behavior of milk protein composite gel for extrusion-based 3D food printing. *LWT, 102*, 338–346. https://doi.org/10.1016/j.lwt.2018.12.053

Liu, Z., Zhang, M., & Bhandari, B. (2018). Effect of gums on the rheological, microstructural and extrusion printing characteristics of mashed potatoes. *International Journal of Biological Macromolecules, 117*, 1179–1187. https://doi.org/10.1016/j.ijbiomac.2018.06.048

Liu, Z. B., Bhandari, B., Prakash, S., Mantihal, S., & Zhang, M. (2019). Linking rheology and printability of a multicomponent gel system of carrageenan-xanthan-starch in extrusion based additive manufacturing. *Food Hydrocolloids, 87*, 413–424. https://doi.org/10.1016/j.foodhyd.2018.08.026

Makroo, H. A., Prabhakar, P. K., Rastogi, N. K., & Srivastava, B. (2019). Characterization of mango puree based on total soluble solids and acid content: Effect on physico-chemical, rheological, thermal and ohmic heating behavior. *LWT, 103*, 316–324. https://doi.org/10.1016/j.lwt.2019.01.003

Meng, F. B., Lei, Y. T., Zhang, Q., Li, Y. C., Chen, W. J., & Liu, D. Y. (2022). Encapsulation of *Zanthoxylum bungeanum* essential oil to enhance flavor stability and inhibit lipid oxidation of Chinese-style sausage. *Journal of the Science of Food and Agriculture, 102*(10), 4035–4045. https://doi.org/10.1002/jsfa.11752

Nie, J., Xue, C., Xiong, S., Yin, T., & Huang, Q. (2024). Comparative analysis of soluble and insoluble dietary fiber on improving the gelation performance and fishy odors of silver carp surimi. *International Journal of Biological Macromolecules, 262*, Article 129938. https://doi.org/10.1016/j.ijbiomac.2024.129938

Ouyang, K., Tao, Q., Xie, H., Wang, W., Shi, W., Shi, Q., & Zhao, Q. (2024). Enrichment of bread with soluble and insoluble rice bran dietary fibers: A comparative study. *Journal of Cereal Science*. https://doi.org/10.1016/j.jcs.2024.103927

Pant, A., Lee, A. Y., Karyappa, R., Lee, C. P., An, J., Hashimoto, M., & Zhang, Y. (2021). 3D food printing of fresh vegetables using food hydrocolloids for dysphagic patients. *Food Hydrocolloids, 114*, Article 106546. https://doi.org/10.1016/j.foodhyd.2020.106546

Sedjoah, R.-C. A.-A., Ma, Y., Xiong, M., & Yan, H. (2021). Fast monitoring total acids and total polyphenol contents in fermentation broth of mulberry vinegar using MEMS and optical fiber near-infrared spectrometers. *Spectrochimica Acta Part A: Molecular and Biomolecular Spectroscopy, 260*, Article 119938. https://doi.org/10.1016/j.saa.2021.119938

Sharma, O. P., & Bhat, T. K. (2009). DPPH antioxidant assay revisited. *Food Chemistry, 113*(4), 1202–1205. https://doi.org/10.1016/j.foodchem.2008.08.008

Sharma, R., Chandra Nath, P., Kumar Hazarika, T., Ojha, A., Kumar Nayak, P., & Sridhar, K. (2024). Recent advances in 3D printing properties of natural food gels: Application of innovative food additives. *Food Chemistry, 432*, Article 137196. https://doi.org/10.1016/j.foodchem.2023.137196

Sun, S. J., Deng, P., Peng, C. E., Ji, H. Y., Mao, L. F., & Peng, L. Z. (2022). Extraction, structure and Immunoregulatory activity of low molecular weight polysaccharide from Dendrobium officinale. *Polymers, 14*(14). https://doi.org/10.3390/polym14142899. Article 2899.

Tarahi, M., Mohamadzade Fakhr-davood, M., Ghaedrahmati, S., Roshanak, S., & Shahidi, F. (2023). Physicochemical and sensory properties of vegan gummy candies enriched with high-Fiber Jaban watermelon exocarp powder. *Foods, 12*(7). https://doi.org/10.3390/foods12071478. article 1478.

Wang, H., Hu, L., Du, J., Peng, L., Ma, L., & Zhang, Y. (2021). Development of rheologically stable high internal phase emulsions by gelatin/chitooligosaccharide mixtures and food application. *Food Hydrocolloids, 121*, Article 107050. https://doi.org/10.1016/j.foodhyd.2021.107050

Wedamulla, N. E., Fan, M., Choi, Y.-J., & Kim, E.-K. (2023a). Combined effect of heating temperature and content of pectin on the textural properties, rheology, and 3D printability of potato starch gel. *International Journal of Biological Macromolecules, 253*, Article 127129. https://doi.org/10.1016/j.ijbiomac.2023.127129

Wedamulla, N. E., Fan, M., Choi, Y.-J., & Kim, E.-K. (2023b). Effect of pectin on printability and textural properties of potato starch 3D food printing gel during cold storage. *Food Hydrocolloids, 137*, Article 108362. https://doi.org/10.1016/j.foodhyd.2022.108362

Wei, C., Zhang, Y., Zhang, H., Li, J., Tao, W., Linhardt, R. J., & Ye, X. (2019). Physicochemical properties and conformations of water-soluble peach gums via different preparation methods. *Food Hydrocolloids, 95*, 571–579. https://doi.org/10.1016/j.foodhyd.2018.03.049

Yan, B., Zhao, Z., Zhang, N., Ruan, H., Yu, X., Zhao, J., & Fan, D. (2022). 3D food printing curing technology based on gellan gum. *Journal of Food Engineering, 327*, Article 111036. https://doi.org/10.1016/j.jfoodeng.2022.111036

Yang, F. L., Guo, C. F., Zhang, M., Bhandari, B., & Liu, Y. P. (2019). Improving 3D printing process of lemon juice gel based on fluid flow numerical simulation. *LWT-Food Science and Technology, 102*, 89–99. https://doi.org/10.1016/j.lwt.2018.12.031

Yu, H., Zhao, Y., Li, R., Guo, X., Liu, P., & Zhang, J. (2024). Effect of apple high-methoxyl pectin on heat-induced gelation of silver carp myofibrillar protein. *Food Chemistry, 441*, Article 138366. https://doi.org/10.1016/j.foodchem.2024.138366

Yu, Q., Zhang, M., Bhandari, B., & Li, J. Y. (2023). Future perspective of additive manufacturing of food for children. *Trends in Food Science & Technology, 136*, 120–134. https://doi.org/10.1016/j.tifs.2023.04.009

Zeng, S., Long, J., Sun, J., Wang, G., & Zhou, L. (2022). A review on peach gum polysaccharide: Hydrolysis, structure, properties and applications. *Carbohydrate Polymers, 279*, Article 119015. https://doi.org/10.1016/j.carbpol.2021.119015

Zhang, J., Li, Y., Cai, Y., Ahmad, I., Zhang, A., Ding, Y., & Lyu, F. (2022). Hot extrusion 3D printing technologies based on starchy food: A review. *Carbohydrate Polymers, 294*, Article 119763. https://doi.org/10.1016/j.carbpol.2022.119763

Zhang, W., Guo, C., Du, M., Hu, X., & Yi, J. (2024). Effects of gel spatial structure and water state on 3D printability: A case study of honey bee pupa protein and soybean dietary fiber. *Food Hydrocolloids, 146*, Article 109224. https://doi.org/10.1016/j.foodhyd.2023.109224

Zhong, G., Meng, F.-B., Li, Y.-C., Liu, D.-Y., Guo, X.-Q., & Zheng, L.-J. (2018). Structure and rheological characterization of konjac glucomannan octenyl succinate (KGOS). *Food Hydrocolloids, 77*, 386–396. https://doi.org/10.1016/j.foodhyd.2017.10.015

Zhou, L., Meng, F.-B., Li, Y.-C., Shi, X.-D., Yang, Y.-W., & Wang, M. (2023). Effect of peach gum polysaccharide on the rheological and 3D printing properties of gelatin-based functional gummy candy. *International Journal of Biological Macromolecules, 253*, Article 127186. https://doi.org/10.1016/j.ijbiomac.2023.127186

Zhou, X., Feng, X., Qi, W., Zhang, J., & Chen, L. (2024). Microencapsulation of vitamin E by gelatin-high/low methoxy pectin complex coacervates: Effect of pH, pectin type, and protein/polysaccharide ratio. *Food Hydrocolloids, 151*, Article 109794. https://doi.org/10.1016/j.foodhyd.2024.109794

Zhu, S., Stieger, M. A., van der Goot, A. J., & Schutyser, M. A. I. (2019). Extrusion-based 3D printing of food pastes: Correlating rheological properties with printing behaviour. *Innovative Food Science & Emerging Technologies, 58*, Article 102214. https://doi.org/10.1016/j.ifset.2019.102214

Zulueta, A., Esteve, M. J., & Frígola, A. (2009). ORAC and TEAC assays comparison to measure the antioxidant capacity of food products. *Food Chemistry, 114*(1), 310–316. https://doi.org/10.1016/j.foodchem.2008.09.033